

Experimental Determination of the Rate Constant of Deactivation of Poly(styrene) and Poly(butyl acrylate) Radicals in Atom Transfer Radical Polymerization

Grégory Chambard,[†] Bert Klumperman,* and Anton L. German

Eindhoven University of Technology, Laboratory of Polymer Chemistry, P.O. Box 513, 5600 MB Eindhoven, The Netherlands

Received September 12, 2001

ABSTRACT: The rate constants of deactivation in atom transfer radical polymerization of styrene and butyl acrylate have been determined. The values are $k_{\text{deact}} = 7 \times 10^7 \text{ L mol}^{-1} \text{ s}^{-1}$ for styrene and $1 \times 10^8 \text{ L mol}^{-1} \text{ s}^{-1}$ for butyl acrylate, both measured in *p*-xylene at 110 °C. The effect of solvent polarity seems to be insignificant on the basis of results measured in butyl acetate. The proper conditions for the experimental determination of k_{deact} were found on the basis of computer simulations. Conditions were chosen such that the sensitivity of the measured rate constants toward experimental conditions and toward uncertainties in other rate parameters was minimal.

Introduction

Atom transfer radical polymerization (ATRP) has proved to be an excellent method to control chain growth and herewith molecular-weight distributions and chemical composition distributions in the (co)polymerization of vinyl monomers. However, few publications have been dedicated to the proper kinetic description of ATRP polymerizations.^{1,2} Fukuda et al.³ determined the activation rate coefficient of a number of dormant species common in ATRP. We recently reported a method to determine this rate coefficient for poly(styrene) and poly(butyl acrylate) dormant species in various solvents.⁴ To the best of our knowledge, there is only one very recent study on the deactivation process.⁵

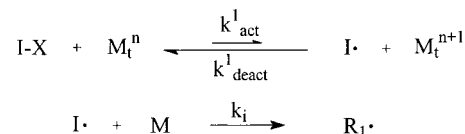
Thorough knowledge on the important kinetic parameters is of paramount importance to control the ATRP copolymerization process. For a proper description of ATRP (co)polymerizations the deactivation rate coefficients are of great significance. In this publication, we propose a straightforward method to determine the deactivation rate coefficient experimentally by the addition of a finite amount of deactivating species at the onset of the ATRP reaction.

Theory

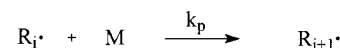
ATRP relies on the reversible deactivation of propagating radicals by a deactivating species, a metal complex in its oxidized form, hereby forming so-called dormant species that can be reactivated later in the polymerization. We can assume a model system, in which only initiation, propagation, and termination reactions occur, as well as activation of dormant species and deactivation of polymeric radicals (Scheme 1). The halide atom (X) is transferred from the dormant species (R_i-X) to the transition-metal complex (M_t^n) and a radical (R_i^\bullet) is formed that is able to add monomer (M). The initiation step in ATRP involves a halide species ($I-X$) and is completely analogous to the activation of dormant species. Termination products are symbolized by D. Transfer reactions and thermal initiation have

Scheme 1. Fundamental Reaction Steps in an ATRP Homopolymerization

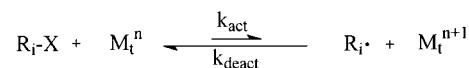
Initiation:



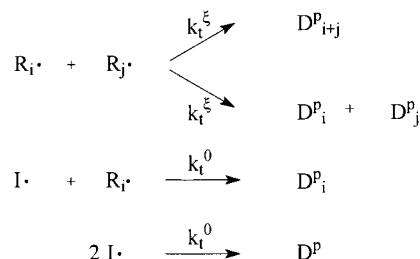
Propagation:



ATRP equilibrium:



Bimolecular termination:



been neglected in this model, and for bimolecular termination by combination and disproportionation both rate coefficients are assumed to be equal.

Here k_{act} and k_{deact} are the activation and deactivation rate coefficients for the dormant species, respectively; k_{act}^1 and k_{deact}^1 are the corresponding parameters for the alkyl halide initiator. Additionally, k_t^ξ symbolizes the conversion-dependent termination rate constant, k_t^0 the termination rate coefficient for species with chain length 1, and k_i the initiation rate coefficient. Finally, k_p is the propagation rate coefficient.

The proposed ATRP process obeys conventional free-radical kinetics, which is supported by numerous data

[†] Current address: Dow Chemical, Terneuzen, The Netherlands.

on ATRP homo- and copolymerizations.^{6–8} As a result, the important reaction steps in an ATRP homopolymerization yield the following mass balances (eqs 1a–1g).

$$\frac{d[I-X]}{dt} = -k_{act}^1[I-X][M_t^n] + k_{deact}^1[I^*][M_t^{n+1}] \quad (1a)$$

$$\frac{d[I^*]}{dt} = k_{act}^1[I-X][M_t^n] - k_{deact}^1[I^*][M_t^{n+1}] - 2k_t^0[I^*]^2 - 2k_t^0[I^*][R^*] - k_i[I^*][M] \quad (1b)$$

$$\frac{d[R^*]}{dt} = k_{act}[R-X][M_t^n] - k_{deact}[R^*][M_t^{n+1}] + k_i[I^*][M] - 2k_t^0[I^*][R^*] - 2k_t^0[R^*]^2 \quad (1c)$$

$$\frac{d[R-X]}{dt} = -k_{act}[R-X][M_t^n] + k_{deact}[R^*][M_t^{n+1}] \quad (1d)$$

$$\frac{d[M]}{dt} = -k_p[R^*][M] - k_i[I^*][M] \quad (1e)$$

$$\frac{d[M_t^n]}{dt} = -k_{act}^1[I-X][M_t^n] + k_{deact}^1[I^*][M_t^{n+1}] - k_{act}[R-X][M_t^n] + k_{deact}[R^*][M_t^{n+1}] \quad (1f)$$

$$\frac{d[M_t^{n+1}]}{dt} = k_{act}^1[I-X][M_t^n] - k_{deact}^1[I^*][M_t^{n+1}] + k_{act}[R-X][M_t^n] - k_{deact}[R^*][M_t^{n+1}] \quad (1g)$$

For an ATRP homopolymerization with $[Cu(I)]_0 = 0$, the rate of reaction can be described by eq 2,^{1,2}

$$-\ln(1 - \xi) = \ln\left(\frac{[M]_0}{[M]}\right) = \frac{3}{2}k_p\left(\frac{k_{act}[I-X]_0[Cu^+]_0}{6k_{deact}k_t^0}\right)^{1/3} t^{2/3} \quad (2)$$

where ξ represents fractional conversion and t = time. When the activation rate coefficients are known, together with literature values of the termination and propagation rate coefficients, the deactivation rate coefficient can be extracted.

The conversion-dependent termination rate coefficient, k_t^0 , can be described by eq 3.^{9–11}

$$k_t^0 = k_t^0\left(1 + \frac{[M]_0}{[I-X]_0}\xi\right)^{-(0.664+2.02w_{M,0}\xi)} \quad (3)$$

However, several problems arise when using this approach. First, the termination rate constant is not well-known for three reasons. The conversion-dependent termination rate constant in principle holds for methyl and butyl methacrylate oligomers in high molar mass methyl and butyl methacrylate matrices.⁹ Furthermore, at elevated temperatures, e.g. at 110 °C, these termination rate constants have not been determined. Finally, in the derivation of the expression of k_t^0 , it has been assumed that the concentration of polymer exceeds c^* , i.e., the concentration at which chains start overlapping. Since in ATRP all chains start growing at the beginning of the reaction, and grow relatively slowly, it takes a while to reach the value of c^* . The diffusion behavior of oligomers as part of a relatively monodisperse matrix is an interesting area of future research.

Another problem arises on recognizing that eq 2 does not take into account the initiation process, i.e., the activation and deactivation of the alkyl halide initiator. In general, one expects somewhat different activation and deactivation rate coefficients of the alkyl halide initiator compared to those of the PS and PBA dormant species, as has already been shown experimentally for the activation rate coefficient.¹²

Experimental Section

Materials. The copper ligand, 4,4'-di-*n*-heptyl-2,2'-bipyridine (dHbpy), was synthesized according to a literature procedure.¹³ Styrene (S, Aldrich, 99%) and butyl acrylate (BA, Aldrich, 99+%) were distilled and stored over molecular sieves. *p*-Xylene (Aldrich, 99+% HPLC grade) was stored over molecular sieves and used without further purification. Stabilized tetrahydrofuran (AR, Biosolve) was used as received. Ethyl 2-bromoisobutyrate (Aldrich, 98%) and CuBr₂ (Aldrich, 99%) were used as received. CuBr (Aldrich, 99.999%) was used as received, stored in a glovebox under a nitrogen atmosphere, and used in the "kinetic experiments". CuBr (Aldrich, 98%) was also used as received and used for the homopolymerizations. Aluminum oxide (activated, neutral, Brockman I, STD grade approximately 150 mesh, 58 Å, Aldrich) was used as received.

Analytical Methods. Monomer conversion was determined by gas chromatography using a HP 5890 gas chromatograph equipped with an AT Wax column (Alltech, length 30 m, film thickness 1.0 μm) and an autosampler. Size exclusion chromatography (SEC) was carried out with a Waters model 510 pump and a Waters 712 WISP using 4 PL-gel mix C columns (300 mm × 7.5 mm, Polymer Laboratories) at 40 °C and tetrahydrofuran as the eluent. The eluent flow rate was 1.0 mL min⁻¹. Calibration was performed with polystyrene standards with narrow molecular weight distributions (Polymer Laboratories). The BA polymers were not corrected with Mark-Houwink parameters from the literature,¹⁴ since molecular weights were too small for the parameters to be applicable. A Waters 410 differential refractometer was used for detection. Data acquisition was done with Millennium-32 3.05 software.

Procedure for Homopolymerizations without Cu(II).

A typical homopolymerization of S was conducted in the following way. In a 100 mL three-necked round-bottom flask equipped with a magnetic stirrer, *p*-xylene (5.00 g) was mixed with S (5.00 g, 0.0480 mol), dHbpy (0.338 g, 9.60 × 10⁻⁴ mol), and ethyl 2-bromoisobutyrate (0.0940 g, 4.82 × 10⁻⁴ mol). While stirring, the reaction mixture was degassed by purging with dry argon for at least 45 min. CuBr (0.0689 g, 4.80 × 10⁻⁴ mol) was added, and the reaction mixture was homogenized and purged with dry argon for another 15 min. After this, the reaction mixture was placed in a thermostatically controlled oil bath at 110 °C. Samples from the reaction mixture were withdrawn through a septum with a syringe and cooled immediately. Monomer conversion was determined by gas chromatography. The remainder of the samples was used for molecular weight analysis. For this purpose, the samples were passed through a column with aluminum oxide to remove the copper catalyst using stabilized tetrahydrofuran as eluent. After subsequent drying, the polymers were dissolved in stabilized tetrahydrofuran at 1 mg mL⁻¹ and filtrated using 0.2 μm filters. The molecular weights were determined by SEC.

Procedure for "Kinetic Experiments" To Determine k_{deact} .

The experimental procedure for the homopolymerizations of S and BA is similar to those described in the previous paragraph. However, to rule out the effects of the initiation process and uncertainties in the chain-length-dependent termination rate coefficient on the course of the reaction, 5% of CuBr₂ based on the total amount of copper was added. Both theory and experiment demonstrate that, above a certain threshold concentration of deactivator ($[Cu(II)]_0$), the conversion vs time behavior changes from a nonlinear to a linear dependence in a semilogarithmic plot.^{15,16} A typical kinetic

Table 1. Initial Concentrations and Parameters Used in the Simulation of the ATRP System As Depicted in Scheme 1

param/ concn	value	param/ concn	value
$[I-X]_0$	$5 \times 10^{-2} \text{ mol L}^{-1}$	k_{deact}^1	$1.1 \times 10^7 \text{ L mol}^{-1} \text{ s}^{-1}$ ^{3,12}
$[M_t^*]_0$	$5 \times 10^{-2} \text{ mol L}^{-1}$	k_p	$1572 \text{ L mol}^{-1} \text{ s}^{-1}$ ¹⁷
$[M]_0$	4.2 mol L^{-1}	k_t^0	$1 \times 10^8 \text{ L mol}^{-1} \text{ s}^{-1}$ ¹⁸
k_{act}	$0.45 \text{ L mol}^{-1} \text{ s}^{-1}$ ³		

experiment with S was performed using the following procedure. In a 100 mL three-necked round-bottom flask, *p*-xylene (5.00 g) was mixed with S (5.00 g, 0.0480 mol), dHbpy (0.338 g, 9.60×10^{-4} mol), CuBr_2 (5.40×10^{-3} g, 2.42×10^{-5} mol), and ethyl 2-bromoisobutyrate (0.0940 g, 4.82×10^{-4} mol). While stirring, the reaction mixture was degassed by purging with dry argon for at least 45 min. CuBr (0.0654 g, 4.56×10^{-4} mol) was added, and the reaction mixture was homogenized and purged with dry argon for another 15 min. After this, the reaction mixture was placed in an oil bath at 110 °C. Samples from the reaction mixture were withdrawn with a syringe through a septum and cooled immediately. Monomer conversion was determined by gas chromatography.

Computer Simulations. Computer simulations of the ATRP system in Scheme 1 were carried out using Mathematica 4.0 software; see the Supporting Information for the code used in the simulations. The values for the different parameters are listed in Table 1.

Results and Discussion

Computer Simulations. Several important notes should be mentioned at this stage. First, transfer reactions and thermal initiation have been neglected, and the rate coefficients for bimolecular termination by combination and disproportionation are assumed to be equal. Second, the termination events involving initiator-derived radicals (I^*) are assumed to be governed by k_t^0 , i.e., the termination rate coefficient for small species. Although the initiation step can be up to 10 times faster than propagation,¹⁹ in the simulations the initiation step is assumed to be as fast as the subsequent propagation steps, i.e., $k_i = k_p$. Finally, the propagation rate coefficient is assumed to be independent of the chain length of the growing radical.

Figure 1a,b demonstrates the effect of inaccuracies in k_{act}^1 and k_{deact}^1 on the course of polymerization.

When the activation and deactivation of the alkyl halide initiator are not accurately known, this leads to large errors in the eventual assessment of the deactivation rate parameter of the dormant species.

Figure 2 shows the effect of inaccuracies in k_t^0 on the evolution of $-\ln(1 - \xi)$ in time.

Simulations of the ATRP system depicted in Scheme 1 and using eqs 1a–1g without an initial amount of deactivator show that inaccuracies in k_t^0 , and therefore in k_t^{ξ} , as well as the initiation process, greatly affect the rate of polymerization.

When a significant amount of deactivating species is present at the onset of the polymerization reaction, e.g., 5% based on total copper, the rate of polymerization becomes independent of relatively large differences in the initiation process and termination rate coefficient (Figures 3 and 4, respectively). The reason for this independence on rate coefficients of (de)activation of the initiator is caused by the larger rate of deactivation. Because of the presence of deactivator (Cu(II)), the deactivation reaction is competing with bimolecular termination from the onset of the reaction. Consequently, the effect of varying rate constants k_{act}^1 and

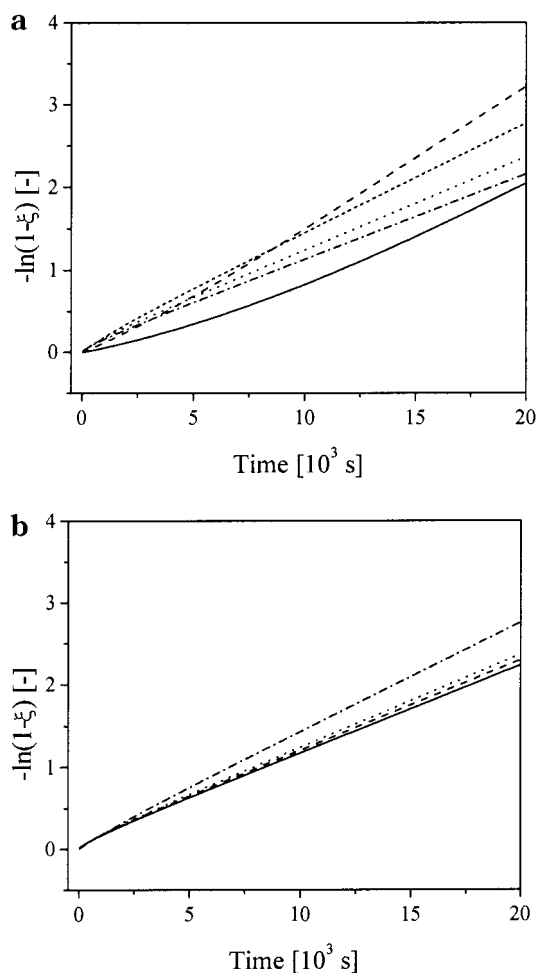


Figure 1. (a) Evolution of $-\ln(1 - \xi)$ in time for different values of k_{act}^1 ; $k_{\text{deact}}^1 = 1.1 \times 10^7 \text{ L mol}^{-1} \text{ s}^{-1}$, $k_{\text{act}}^1 = 0.001 \text{ L mol}^{-1} \text{ s}^{-1}$ (—), $0.01 \text{ L mol}^{-1} \text{ s}^{-1}$ (---), $0.1 \text{ L mol}^{-1} \text{ s}^{-1}$ (- - -), $0.45 \text{ L mol}^{-1} \text{ s}^{-1}$ (···), and $1 \text{ L mol}^{-1} \text{ s}^{-1}$ (- · - ·). Other parameters as in Table 1. (b) Evolution of $-\ln(1 - \xi)$ in time for different values of k_{deact}^1 ; $k_{\text{act}}^1 = 0.45 \text{ L mol}^{-1} \text{ s}^{-1}$, $k_{\text{deact}}^1 = 1.1 \times 10^6 \text{ L mol}^{-1} \text{ s}^{-1}$ (—), $5 \times 10^6 \text{ L mol}^{-1} \text{ s}^{-1}$ (---), $1.1 \times 10^7 \text{ L mol}^{-1} \text{ s}^{-1}$ (···), and $1 \times 10^8 \text{ L mol}^{-1} \text{ s}^{-1}$ (- · - ·). Other parameters as in Table 1.

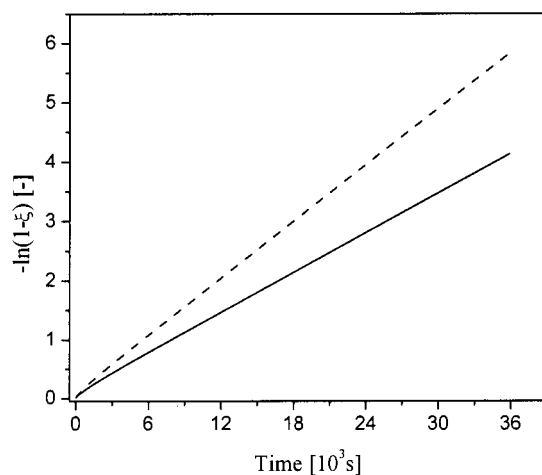


Figure 2. Evolution of $-\ln(1 - \xi)$ in time as a function of k_t^0 in the absence of Cu(II) ; $k_t^0 = 1 \times 10^8 \text{ L mol}^{-1} \text{ s}^{-1}$ (—); $k_t^0 = 5 \times 10^7 \text{ L mol}^{-1} \text{ s}^{-1}$ (---).

k_{deact}^1 is negligible when realistic values for the rate constants are chosen.

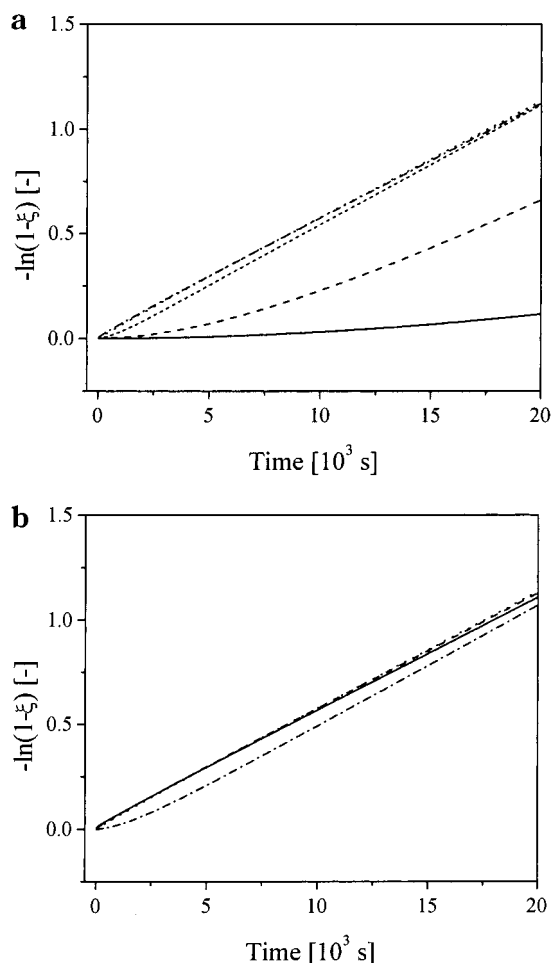


Figure 3. (a) Evolution of $-\ln(1 - \xi)$ in time for different values of k_{act}^1 ; $k_{\text{deact}}^1 = 1.1 \times 10^7 \text{ L mol}^{-1} \text{ s}^{-1}$ and $[\text{Cu(II)}]_0 = 2.5 \times 10^{-3} \text{ mol L}^{-1}$; $k_{\text{act}}^1 = 0.001 \text{ L mol}^{-1} \text{ s}^{-1}$ (—), $0.01 \text{ L mol}^{-1} \text{ s}^{-1}$ (---), $0.1 \text{ L mol}^{-1} \text{ s}^{-1}$ (- - -), $0.45 \text{ L mol}^{-1} \text{ s}^{-1}$ (···), and $1 \text{ L mol}^{-1} \text{ s}^{-1}$ (- · -). Other parameters as in Table 1. (b) Evolution of $-\ln(1 - \xi)$ in time for different values of k_{deact}^1 ; $k_{\text{act}}^1 = 0.45 \text{ L mol}^{-1} \text{ s}^{-1}$ and $[\text{Cu(II)}]_0 = 2.5 \times 10^{-3} \text{ mol L}^{-1}$; $k_{\text{deact}}^1 = 1.1 \times 10^6 \text{ L mol}^{-1} \text{ s}^{-1}$ (—), $5 \times 10^6 \text{ L mol}^{-1} \text{ s}^{-1}$ (···), $1.1 \times 10^7 \text{ L mol}^{-1} \text{ s}^{-1}$ (- - -), and $1 \times 10^8 \text{ L mol}^{-1} \text{ s}^{-1}$ (- · -). Other parameters as in Table 1.

As can be seen in Figure 3a, the effect of the activation of the alkyl halide initiator has been drastically diminished. There still is a threshold of approximately $0.1 \text{ L mol}^{-1} \text{ s}^{-1}$, above which k_{act}^1 should be in order to minimize the effect on the course of polymerization. This threshold value is very low, and it is expected that in real ATRP systems k_{act}^1 is higher. For 1-phenylethyl bromide, for instance, the k_{act}^1 equals $0.45 \text{ L mol}^{-1} \text{ s}^{-1}$,²⁰ which implies that in this case the initiation of the alkyl halide initiator should not influence the rate of polymerization. The same holds for k_{deact}^1 , since Figure 3b shows that the rate of polymerization is not affected when this deactivation rate coefficient is not too high. Even for the highest value of k_{deact}^1 the deviations from the other curves in Figure 3b are not extremely large. Experimentally, this deactivation rate coefficient is calculated from rate data for ATRP homopolymerizations of S in diphenyl ether, in combination with information on the activation rate coefficient, and was found to be $1.1 \times 10^7 \text{ L mol}^{-1} \text{ s}^{-1}$.^{3,13} Analogously, the effect of inaccuracies in k_{t}^0 on the course of the polymerization can be minimized by the presence

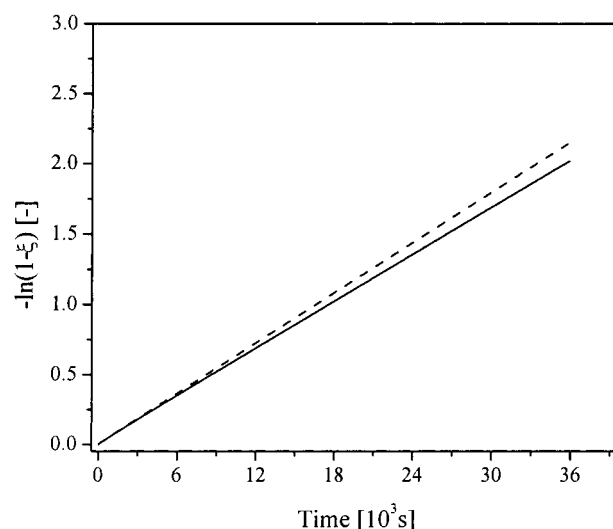


Figure 4. Evolution of $-\ln(1 - \xi)$ in time as a function of k_{t}^0 with 5% of Cu(II); $k_{\text{t}}^0 = 1 \times 10^8 \text{ L mol}^{-1} \text{ s}^{-1}$ (—); $k_{\text{t}}^0 = 5 \times 10^7 \text{ L mol}^{-1} \text{ s}^{-1}$ (---).

of 5% deactivating species at the onset of polymerization (Figure 4).

However, this implies that eq 2 no longer applies and that eq 4 has to be used to assess the evolution of $-\ln(1 - \xi)$ with time.¹

$$-\ln(1 - \xi) = \ln\left(\frac{[\text{M}]_0}{[\text{M}]}\right) = k_{\text{p}} \frac{k_{\text{act}}}{k_{\text{deact}}} \frac{[\text{R-X}]_0 [\text{M}_{\text{t}}^n]_0}{[\text{M}_{\text{t}}^{n+1}]_0} t \quad (4)$$

Homopolymerizations without Cu(II). The results for the S and BA homopolymerizations are summarized in Figure 5, a and b, respectively, where $-\ln(1 - \xi)$ is plotted vs time.

Since no CuBr₂ was added, the experimental data in Figure 5 have been fitted to eq 2 assuming a constant termination rate coefficient; the data are well described. To describe the kinetics of living radical polymerization, the use of conversion-dependent and chain-length-dependent rate coefficient does not seem to be necessary. A probable explanation for this apparent deviation from classical free radical polymerization kinetics is the completely different evolution of molar mass and reaction mixture viscosity between the two systems. Furthermore, the ATRP system that we used for these homopolymerizations made use of (only) 98% pure CuBr, and therefore 2% of Cu(II) species was present from the very start of the reaction. Apparently, 2% of Cu(II) species does not influence the kinetics to a large extent. This observation agrees well with earlier theory¹⁵ and experimental¹⁶ work that indicated that the addition of small amounts of Cu(II) does not change the kinetic regime of the reaction. In an experimental example on the ATRP of MMA as much as 10% of Cu(II) relative to Cu(I) had to be added before the persistent radical effect was no longer visible in conversion vs time data.¹⁶

Kinetic Experiments. The evolution of $-\ln(1 - \xi)$ in time for duplicate homopolymerizations of S and BA is displayed in parts a and b of Figure 6, respectively. The differences between the evolutions of $-\ln(1 - \xi)$ for the duplicate reactions are caused by differences in $[\text{I-Br}]_0$, $[\text{Cu(I)}]_0$, and $[\text{Cu(II)}]_0$ (see Table 2).

The data in Figures 6 show that eq 4 is obeyed, although the BA homopolymerizations are less scat-

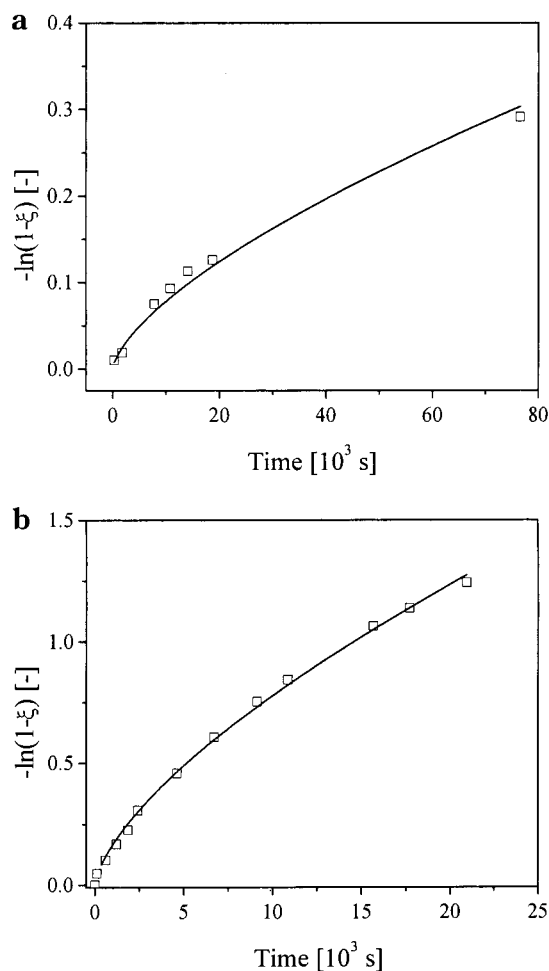


Figure 5. (a) Evolution of $-\ln(1-\xi)$ in time for a homopolymerization of S in *p*-xylene at 110 °C. (b) Evolution of $-\ln(1-\xi)$ in time for a homopolymerization of BA in *p*-xylene at 110 °C.

tered. This is most probably due to the smaller amount of Cu(II) needed for the transition from nonlinear to linear behavior in the case of BA compared to S. According to eq 4, to calculate the deactivation rate coefficients for PS and PBA dormant species, the initial concentrations of alkyl halide initiator, $[I-Br]_0$, catalyst, $[Cu(I)]$, and deactivator, $[Cu(II)]$, need to be known. For both the S homopolymerizations and the BA homopolymerizations, the initial concentrations are collected in Table 2, together with the slopes (α) of the linear fits from Figures 4 and the calculated deactivation rate coefficients, k_{deact}^S and k_{deact}^{BA} .

Table 2 shows that the deactivation rate coefficients for PS and PBA dormant species in *p*-xylene can be

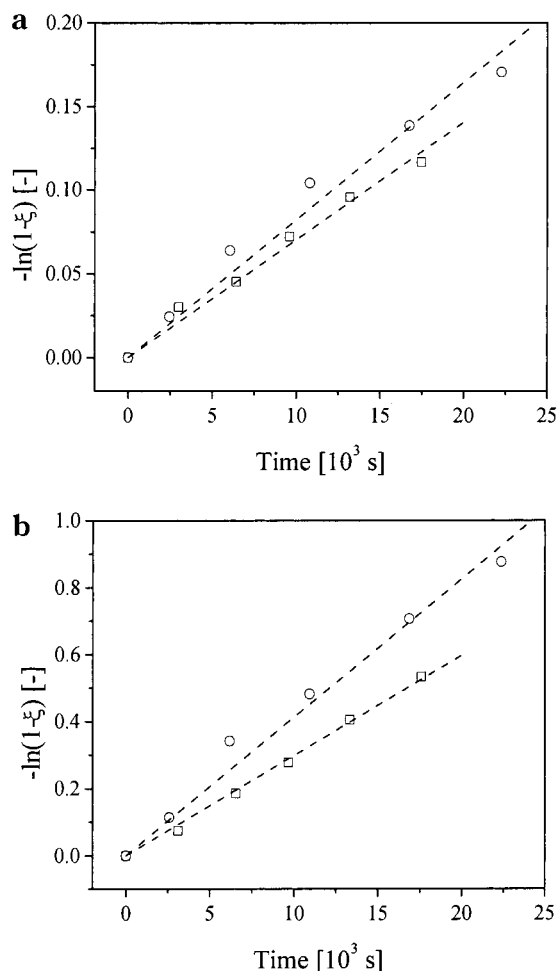


Figure 6. (a) Evolution of $-\ln(1-\xi)$ in time for a homopolymerization of S in *p*-xylene at 110 °C in the presence of 5% of Cu(II); reactions 1 (\square) and 2 (\circ). (b) Evolution of $-\ln(1-\xi)$ in time for a homopolymerization of BA in *p*-xylene at 110 °C in the presence of 5% of Cu(II); reactions 1 (\square) and 2 (\circ).

derived with a reasonable error interval of 10–15%. To investigate the effect of solvent on the deactivation rate coefficients, the kinetic experiments were also carried out in butyl acetate. This is particularly important in view of the copolymerizations of S and BA, where composition drift occurs during polymerization.²¹ The results for the kinetic experiments in butyl acetate are summarized in Table 3. The experimental values of k_{deact} from the present study are in good agreement with previously published values.^{3,22–24}

We assume that the propagation rate coefficient, k_p , is not dependent on solvent. The calculated deactivation rate coefficients from Table 3 do not show a significant

Table 2. Calculated Deactivation Rate Coefficients for S and BA Homopolymerizations in *p*-Xylene at 110 °C in the Presence of 5% Cu(II)

reaction	$[I-Br]_0$, mol L ⁻¹	$[Cu(I)]_0$, mol L ⁻¹	$[Cu(II)]_0$, mol L ⁻¹	α	k_{act} , mol L ⁻¹ s ⁻¹	k_p , mol L ⁻¹ s ⁻¹	k_{deact} , mol L ⁻¹ s ⁻¹
S 1	4.10×10^{-2}	3.89×10^{-2}	2.14×10^{-3}	7.03×10^{-6}	0.43	1.58×10^3	7.2×10^7
S 2	4.19×10^{-2}	3.95×10^{-2}	2.18×10^{-3}	8.22×10^{-6}	0.43	1.58×10^3	6.3×10^7
BA 1	3.71×10^{-2}	3.43×10^{-2}	2.02×10^{-3}	3.18×10^{-5}	0.075	7.84×10^4	1.2×10^8
BA 2	3.91×10^{-2}	3.47×10^{-2}	2.21×10^{-3}	4.13×10^{-5}	0.075	7.84×10^4	8.7×10^7

Table 3. Calculated Deactivation Rate Coefficients for S and BA Homopolymerizations in Butyl Acetate at 110 °C in the Presence of 5% Cu(II)

reaction	$[I-Br]_0$, mol L ⁻¹	$[Cu(I)]_0$, mol L ⁻¹	$[Cu(II)]_0$, mol L ⁻¹	α	k_{act} , mol L ⁻¹ s ⁻¹	k_p , mol L ⁻¹ s ⁻¹	k_{deact} , mol L ⁻¹ s ⁻¹
S	4.35×10^{-2}	3.96×10^{-2}	2.09×10^{-6}	6.37×10^{-6}	0.27	1.58×10^3	5.5×10^7
BA	3.82×10^{-2}	3.61×10^{-2}	1.76×10^{-3}	5.50×10^{-5}	0.086	7.84×10^4	1.1×10^8

solvent dependence. The deactivation rate coefficient for PBA dormant species does not even show the slightest decrease upon employing a more polar solvent, whereas the activation rate coefficient did.⁴ The equivalent coefficient for PS dormant species seems to be somewhat lower than in *p*-xylene but is still very close. The deactivation process is therefore less solvent dependent than the activation process.

To confirm the validity of the present approach for determining the rate constant of deactivation, we re-examine the results shown in Figure 5. The experiments in Figure 5 obey eq 2. Via least-squares analysis, we can determine the proportionality factors relating $-\ln(1 - \xi)$ to $t^{2/3}$ for styrene and for butyl acrylate. The only unknown rate coefficient in eq 2 is then k_t , which can consequently be estimated via this procedure. We obtain single, chain-length-independent, termination rate coefficients for styrene and for butyl acrylate equal to 6×10^9 and $6 \times 10^{10} \text{ L mol}^{-1} \text{ s}^{-1}$, respectively. This approach estimates k_t with a reasonably large error, due to error propagation from the uncertainties in the rate coefficients and reactant concentrations. The fact that we observe a good fit to the experimental data with a chain-length-independent rate coefficient for termination confirms the need for a study of diffusion behavior of oligomers in an oligomers matrix rather than in a high molar mass polymer matrix.

Conclusions

The deactivation rate coefficients have been determined by performing ATRP homopolymerizations in the presence of an initial amount of CuBr_2 . Simulations of the ATRP system show that 5% based on total weight of copper should result in straight plots of $-\ln(1 - \xi)$ vs time. Upon addition of this finite initial amount of deactivating species, the impact of inaccuracies in termination rate coefficients as well as activation and deactivation rate coefficients of the alkyl halide initiator is minimized. The deactivation rate coefficients are similar for PS^\bullet and PBA^\bullet radicals and seem to be less dependent on solvent than the activation rate coefficient.

Acknowledgment. The authors thank Prof. H. Fischer for constructive and inspiring discussions on the modeling of ATRP reactions.

Supporting Information Available: Code for Mathematica 4.0 simulations of ATRP homopolymerization. This

material is available free of charge via the Internet at <http://pubs.acs.org>.

References and Notes

- (1) Fukuda, T.; Goto, A.; Ohno, K. *Macromol. Rapid Commun.* **2000**, *21*, 151–165.
- (2) Fischer, H. *Macromolecules* **1997**, *30*, 5666–5672.
- (3) Ohno, K.; Goto, A.; Fukuda, T.; Xia, J.; Matyjaszewski, K. *Macromolecules* **1998**, *31*, 2699–2701.
- (4) Chambard, G.; Klumperman, B.; German, A. L. *Macromolecules* **2000**, *33*, 4417–4421.
- (5) Matyjaszewski, K.; Paik, H.-j.; Zhou, P.; Diamanti, S. J. *Macromolecules* **2001**, *34*, 5125–5131.
- (6) Haddleton, D. M.; Crossman, M. C.; Hunt, K. H.; Topping, C.; Waterson, C.; Suddaby, K. G. *Macromolecules* **1997**, *30*, 3992–3998.
- (7) Wang, J. S.; Matyjaszewski, K. *Macromolecules* **1995**, *28*, 7572–7573.
- (8) Chambard, G.; Klumperman, B. In *Controlled/Living Radical Polymerization*; Matyjaszewski, K., Ed.; ACS Symposium Series No. 768; American Chemical Society: Washington, DC, 2000; p 197.
- (9) Griffiths, M. C.; Strauch, J.; Monteiro, M. J.; Gilbert, R. G. *Macromolecules* **1998**, *31*, 7835–7844.
- (10) Piton, M. C.; Gilbert, R. G.; Chapman, B. E.; Kuchel, P. W. *Macromolecules* **1993**, *26*, 4472–4477.
- (11) Chambard, G. Ph.D. Thesis, Technische Universiteit Eindhoven, Eindhoven, 2000; p 67.
- (12) Goto, A.; Fukuda, T. *Macromol. Rapid Commun.* **1999**, *20*, 633–636.
- (13) Matyjaszewski, K.; Patten, T. E.; Xia, J. *J. Am. Chem. Soc.* **1997**, *119*, 674–680.
- (14) Hutchinson, R. A.; Paquet, D. A.; McMinn, J. H.; Beuermann, S.; Fuller, R. E.; Jackson, C. *DEHEMA Monogr.* **1995**, *131*, 467.
- (15) Souaille, M.; Fischer, H. *Macromolecules* **2002**, *35*, 248–261.
- (16) Zhang, H.; Klumperman, B.; Ming, W.; Fischer, H.; van der Linde, R. *Macromolecules* **2001**, *34*, 6169–6173.
- (17) Buback, M.; Gilbert, R. G.; Hutchinson, R. A.; Klumperman, B.; Kuchta, R.-D.; Manders, B. G.; O'Driscoll, K. F.; Russell, G. T.; Schweer, J. *Macromol. Chem. Phys.* **1995**, *196*, 3267–3280.
- (18) De Kock, J. B. L. Ph.D. Thesis, Technische Universiteit Eindhoven, Eindhoven, 1999.
- (19) Moad, G.; Rizzardo, E.; Solomon, D. H.; Beckwith, A. L. J. *Polym. Bull. (Berlin)* **1992**, *29*, 647–652.
- (20) Goto, A.; Fukuda, T. *Macromol. Rapid Commun.* **1999**, *20*, 633–636.
- (21) Arehart, S. V.; Matyjaszewski, K. *Macromolecules* **1999**, *32*, 2221–2231.
- (22) Matyjaszewski, K.; Paik, H.-j.; Zhou, P.; Diamanti, S. J. *Macromolecules* **2001**, *34*, 5125–5131.
- (23) Kochi, J. K.; Bemis, A.; Jenkins, C. L. *J. Am. Chem. Soc.* **1968**, *90*, 4616–4625.
- (24) Kochi, J. K.; Subramanian, R. V. *J. Am. Chem. Soc.* **1965**, *87*, 4855–4866.

MA011623F